Reducing p-doping of tin-halide perovskites by trivalent cation doping

Luca Gregori,[a] Chiara Frasca,[b] Daniele Meggiolaro,[c] Paola Belanzoni,[a,c] Muhammad Waqar Ashraf,[d] Artem Musiienko,[b] Antonio Abate,[b,f] * Filippo De Angelis[a,d,e] *

[a] *Department of Chemistry, Biology and Biotechnology, University of Perugia, Via Elce di Sotto 8, 06123, Perugia, Italy.*

[b] *Helmholtz-Zentrum Berlin für Materialien und Energie GmbH, Hahn-Meitner Platz 1, 14109 Berlin, Germany*

[c] *Computational Laboratory for Hybrid/Organic Photovoltaics (CLHYO), Istituto CNR di Scienze e Tecnologie Chimiche "'Giulio Natta"' (CNR-SCITEC), Via Elce di Sotto 8, 06123 Perugia, Italy.*

[d] *Department of Mechanical Engineering, College of Engineering, Prince Mohammad Bin Fahd University, P.O. Box 1664, Al Khobar, 31952, Saudi Arabia.*

[e] *SKKU Institute of Energy Science and Technology (SIEST) Sungkyunkwan University, Suwon, Korea 440-746.*

[f] *Department of Chemical, Materials and Production Engineering, University of Naples Federico II, Piazzale Tecchio 80, 80125 Fuorigrotta, Italy.*

Corresponding Authors

Antonio Abate – antonio.abate@helmholtz-berlin.de

Filippo De Angelis – filippo@thch.unipg.it

Abstract

We investigate trivalent doping of tin-halide perovskites as a means to decrease p-doping and controlling defect activity. Through density functional theory calculations and experimental characterization, we demonstrate that doping with scandium, lanthanum and cerium successfully accomplishes Fermi level upshift, reducing background carrier concentration and defect densities, thereby improving material performance. Solar cells fabrication and testing highlights the efficacy of doping, with scandium delivering increase photocurrent and open circuit voltage compared to control devices, despite being non optimized. This research underscores the potential of cation doping in enhancing the functionality of p-doped tin perovskites for advanced optoelectronic applications.

TOC graphics
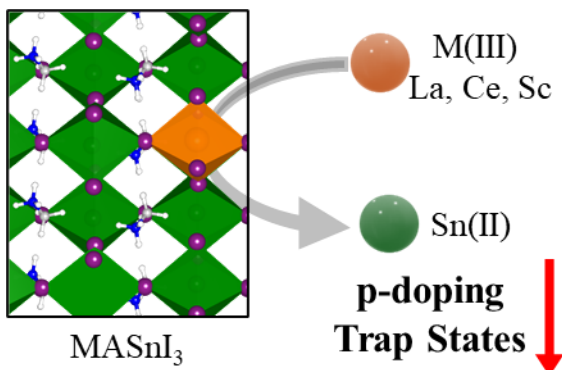
The remarkable optoelectronic features of metal-halide perovskites[1-4] led to photovoltaic efficiency matching that of silicon solar cells.[5] Fervent research is still carried out to stabilize lead-based compounds for single junction and tandem applications;[6-8] and, on a longer time scale, to replace lead with tin.[9,10] The easy oxidation of Sn(II) to Sn(IV) combined with the high p-doping severely restricts the efficiency of tin halide perovskites (THPs), which may otherwise exhibit optoelectronic properties similar or even superior to those of their lead counterpart.[9,11] Tin vacancies (V_{Sn}) and iodine interstitials (I_i), two stable THPs acceptor defects, are the source of native p-doping in THPs[12] which induce background charge density exceeding 10^{19} cm^{-3}. The inclusion of Sn(IV) species into the developing perovskite, likely caused by precursor oxidation, may further introduce trap states and aggravate p-doping.[13] Since the pioneering paper by Kanatzidis and coworkers,[4] SnF$_2$ has been added to the perovskite precursors to limit THP oxidation. Milot et al.[11] found that SnF$_2$ addition inhibited tin oxidation, promoting more crystalline and less p-doped THPs films. SnF$_2$ creates a tin-rich environment which may to some extent limit the formation of tin vacancies; it was also proposed to sequester Sn(IV) species from the precursor solution,[14] thus preventing Sn(IV) from being integrated into the perovskite.[15] The high p-doping of THPs implies short-lived charge carriers, which limit the short circuit photocurrent (J_{SC}) in solar cell devices; trap assisted recombination may, instead, limit the open circuit voltage (V_{OC}).[16] THPs-based solar cells efficiency is currently at ~15%.[17a] (2024:15.14%) The photovoltaic parameters for a prototype champion device (J_{SC}=20.6 mA·cm^{-2}, V_{OC}=0.91 V, and FF=77.1%) (2024: J_{SC}=29.84 mA·cm^{-2}, V_{OC}=0.82 V, and FF=73.58%), indicate that the V_{OC} to band-gap (~1.25 eV) loss can show comparable values to those of optimized lead-based devices (~0.3/0.4 eV).[17] Although J_{SC} has significantly improved in recent record devices,[17b] its value still falls significantly short of what can be predicted based on the optical band gap. Efficiency improvement mainly stands in controlling THPs crystal growth and in mastering electrical properties and defect induced doping. Two strategies can be envisioned to alleviate p-doping in THPs: *i)* the use of molecular n-dopants, capturing holes via dissociative host bonding;[18] and *ii)* extrinsic doping with positively charged species, such as trivalent metal ions,

3

potentially diminishing the hole density by compensating for negatively charged acceptor defects. Molecular doping was recently shown to lead to *ca.* an order of magnitude reduction in background charge density, but this strategy is likely limited to surface and grain boundaries.[18] The intricate impact of extrinsic metal doping has been the subject of computational investigations on lead-based perovskites.[19–23] Lyons investigated doping with different heterovalent metals, both substitutional and interstitial, finding that scandium exhibited favorable exchange energetics with lead.[22] Significantly, Sc(III) doping did not introduce states in the perovskite band gap,[22] contrary to *e.g.* Bi(III) doping.[24] Prior studies on THPs showed that isovalent alloying of the metal site with alkaline and transition metals, such as calcium and cadmium, may raise the formation energy of tin vacancies, limiting p-doping and tin oxidation.[12] Here we examine the impact of trivalent metal doping in THPs using density functional theory (DFT) simulations combined with dedicated experiments to check the impact of the proposed strategy on the optoelectronic materials properties and on solar cell device performance. We find that scandium, cerium and lanthanum may favorably interact with THPs, reducing p-doping and leading to increased device performance. Although our study is based on a partial metal screening and on non-optimized devices, it shows the potential of trivalent metal doping in alleviating p-doping, and likely increasing the stability, of tin-based perovskites.

Among possible trivalent metals, our DFT analysis has been focused on lanthanum, cerium, and scandium, with the goal of reducing p-doping while mitigating the negative effects related to inclusion of deep-level traps.[21] The incorporation of the three dopants has been simulated in the prototype MASnI$_3$ perovskite at the HSE06-SOC level of theory (see Supporting Information for additional computational details), by assessing the dopant incorporation energy, the stable charge states against the Fermi level, and the dopant effect on the carrier density. We studied the defect formation energy (DFE) of the three dopants in substitutional position to tin, Figure 1a, which is expected to be the thermodynamically favored pathway.[22] Figure 1b shows the calculated DFEs

under iodine-medium condition, mimicking stoichiometric perovskite growth. The Fermi level varies within the MASnI$_3$ band gap, here calculated at 1.08 eV, reasonably matching the experimental value of 1.2 eV.[25] We expect minor variations with different A-site cations, such as FA or mixed cation perovskites. As previously reported,[12] the most stable native defects in iodine medium conditions are negatively charged tin vacancies (V_{Sn}^{2-}) followed by negatively charged iodine interstitials (I_i^-). Due to the instability of compensating positively charged defects, such as interstitial tin (Sn_i^{2+}) and iodine vacancy (V_I^+), the Fermi level is pinned at the valence band maximum (VBM), delivering a strongly p-doped material.[12,13] The investigated M(III) dopants are stable in the +3 charge state (the overall supercell charge is +1, due to trivalent cation replacing divalent tin ion) across the entire Fermi level. Thermodynamic ionization levels (TILs), Figure 1c, confirm the shallow nature of the (+/0) transitions, associated to electron capture by the doped perovskite, indicating that these dopants do not introduce recombination levels in the perovskite band-gap.
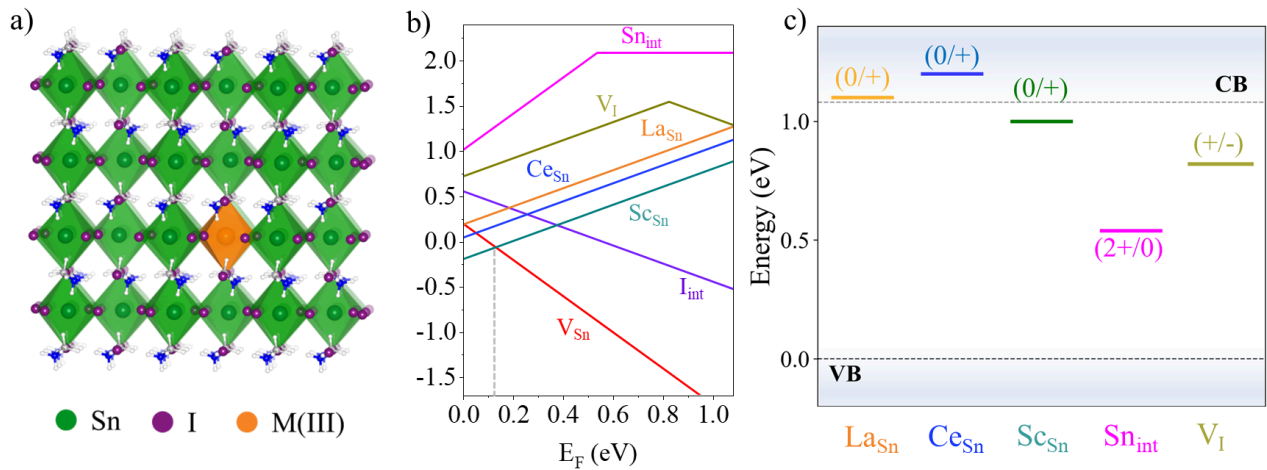

Figure 1. a) Crystal structure of the doped MASnI$_3$ perovskite. M(III) = La, Ce, Sc. The reported structure is a 3x3x2 supercell for visualization b) Defect formation energies (DFEs, eV) calculated at the HSE06-SOC level of theory in iodine-medium conditions for the examined dopants. The DFE of the most stable V_{Sn}^{2-}, I_i^-, V_I and Sn_i native defects are also reported. Dotted gray line indicates the

position of the Fermi level. c) Thermodynamic ionization levels for the examined dopants and the most stable donor defects, V_I and Sn_{int}.

The lanthanum-doped perovskite shows calculated La-I distances of 3.12/3.13 Å, only slightly larger than average Sn-I distances (3.11 Å), see Table S1. The smaller scandium cation introduces a contraction in Sc-I distances (2.92/2.93 Å) but in both La and Sc cases the equatorial and axial distances are comparable. Ce doping, instead, introduces a significant elongation of equatorial Ce-I bonds compared to axial ones (3.32 vs. 3.12 Å, respectively). The investigated dopants show a formation energy lower or equal to that of tin vacancies for Fermi energy equal to zero, *i.e.* at the VBM, Figure 1b. Tin substitution with trivalent ions is thus able to raise the Fermi level away from the VBM, reducing p-doping. Notably, calculated tin substitution energetics of 0.18, 0.04 and -0.19 eV respectively for La, Ce and Sc correlate with trends in ionic radii (La> Ce > Sc). Sc doping shows the most favorable energetics leading to a Fermi level upshift of 0.16 eV above the VBM (0.04 and 0.06 eV for La and Ce respectively), with an associated decrease of the hole density of about one order of magnitude, from $\sim 10^{18}$ to $\sim 10^{17}$ cm^{-3}, Table 1, see Eq. S3. The Fermi level upshift significantly reduces the density of deep defects acting as electron traps, Table 1, thereby deactivating non-radiative recombination pathways. It is worth to mention that the decrease in the hole density achieved by trivalent doping is coupled, however, to an increase of the ionic disorder, as indicated by the negative DFEs obtained for V_{Sn}^{2-} at the Fermi levels of the doped systems. The increased density of tin vacancies may thus limit to some extent the doping ability of these ions compared to theoretical predictions, by impacting the crystallinity of the material unless additional compensation pathways come into play.

Table 1. Calculated density of holes and of V_I and Sn_{int} donor defects for both native and Sc-doped MASnI$_3$ in iodine-medium conditions.

Density (cm^{-3})	Native ($E_F = 0.04$ eV)	Sc-doped ($E_F = 0.16$ eV)
holes	2.9x10^{18}	1.2 x10^{17}
V$_I$	2.8x10^{10}	1.1x10^9
Sn$_{int}$	2.4x10^5	3.8x10^3

It is also interesting to notice that the perovskite incorporation energetics and thus the doping efficiency of such trivalent metal ions may depend on their precursor chemistry. Taking lanthanum as a test case, we simulated the incorporation of trivalent La starting from LaI$_3$ and LaF$_3$ precursors. Our results, see Table S2, show markedly less favorable thermodynamics for La incorporation into the perovskite in the latter case, owing to the increased stability of fluoride lanthanide salts.

To validate the modeling studies, we conducted experiments on tin-based perovskite films doped with the examined trivalent cations. We evaluate their impact on optoelectronic, electrical, and morphological properties, as well as their influence on overall device performance. The FA$_{0.78}$MA$_{0.2}$EDA$_{0.02}$SnI$_3$ perovskite, used as control, was prepared according to our previous publication,[26] and solutions of 0.1M LaI$_3$, CeI$_3$ and ScI$_3$ were mixed with the control solution to produce the three doped variants.
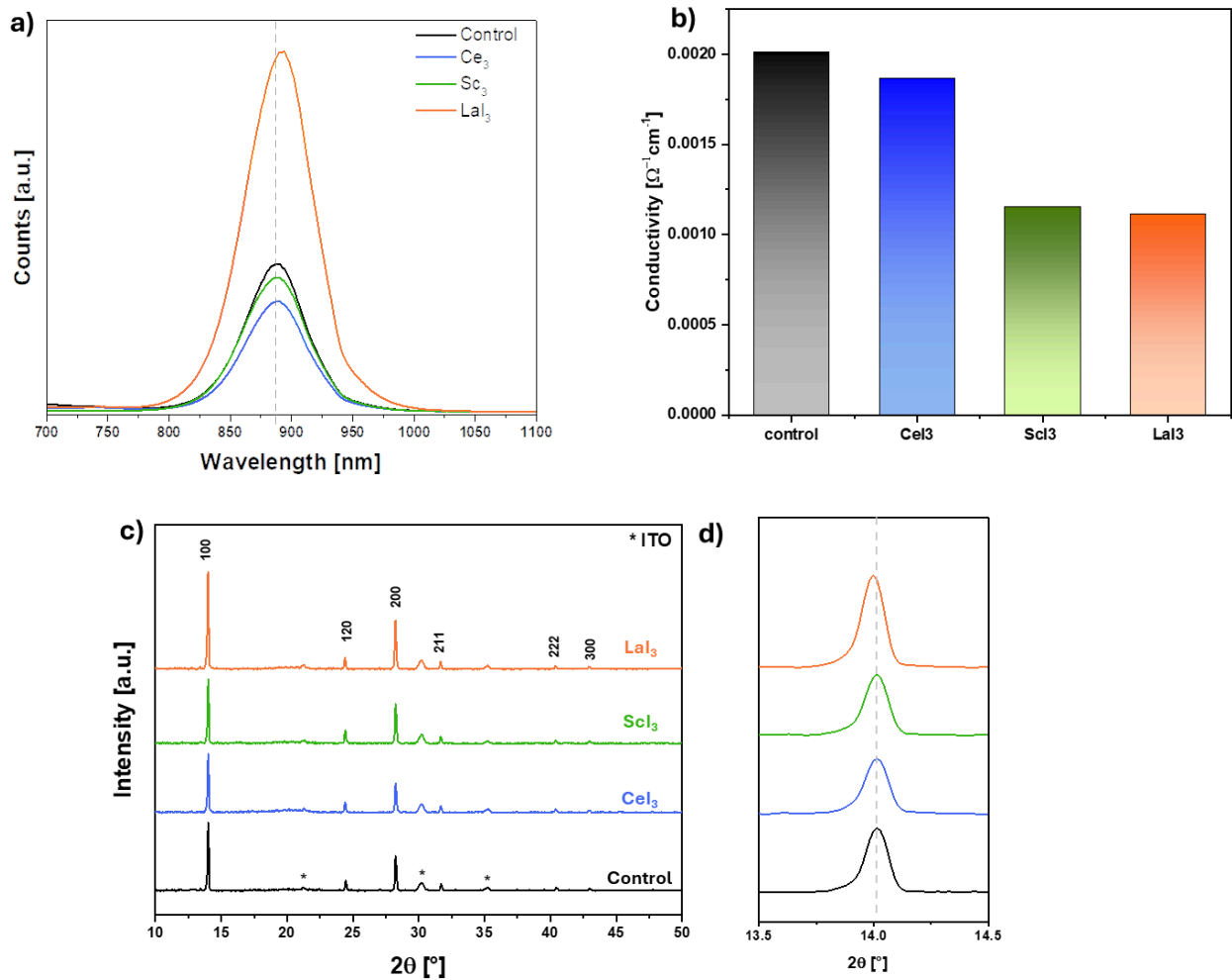
Figure 2. a) Steady-State PL b) Conductivity measurements and c) XRD pattern of control and doped samples; d) insights of the XRD peak at the 100 plane. The grey dotted line is centered on the peak position of the control samples.

We first analyze the optoelectronic properties of the absorber materials. In Figure 2a the steady-state photoluminescence (PL) of the films under investigation, deposited on glass, is shown. The CeI_3 and ScI_3 doped samples demonstrated a similar (slightly lower) PL intensity compared to control, in accordance with our hypothesis that the chosen dopants do not introduce trap states possibly impacting on the luminescence of the material. Interestingly, the addition of LaI_3 doubled the PL intensity, suggesting a reduction of non-radiative charge recombination. We also observed shift of

the PL peak position towards higher energy, which accordingly to the Burstein-Moss effect, can be linked to a reduction of the hole density[27,28] and shallow traps concentration. To compare the difference in the self p-doping level due to the addiction of the trivalent cations, we measured the conductivity of the samples, Figure 2b. The conductivity is proportional to the concentration of the majority carrier which, in the THPs case, corresponds to the free hole density.[29] The observed reduction in conductivity, as evidenced in the case of ScI_3 and LaI_3 doping, aligns with the predictions from DFT calculations, indicating a decrease in self p-doping by passivation of V_{Sn}^{2-} defects.

To investigate the crystallinity of the perovskite films Bragg Brentano X-ray diffraction (XRD) measurements were conducted, the resulting pattern is depicted in Figure 2c. The characteristic peaks at 2θ correspond to the orthorhombic system of FASnI3,[30] with no formation of new phases evident in the doped pattern, as indicated by the absence of additional peaks. Further analysis using Scanning Electron Microscopy (SEM), Figure S3, revealed a decrease in the size of crystal grains in the sample doped with CeI_3, which is reflected in the XRD pattern by a decreased peak intensity. The LaI_3 doped sample exhibited, instead, an increase in peak intensity. Notably, as shown in the enlargement in Figure 2d), which represent the peak located at 2θ ≈ 14.01°, is evident a shift of the pattern towards lower angles with the addition of LaI_3. This shift could be attributed to the reduction of Sn vacancies and the subsequent increase in lattice constant.[31] For the ScI_3 doped sample no significant difference in the crystal structure was observed. Probably, the combined effect of different morphology and degree of crystallinity hinders the observation of lattice variation. Also, despite DFT predicting Sc to be favorably incorporated into the perovskite, we cannot rule out this dopant to be mainly located at the surface, given its smaller ionic radius.
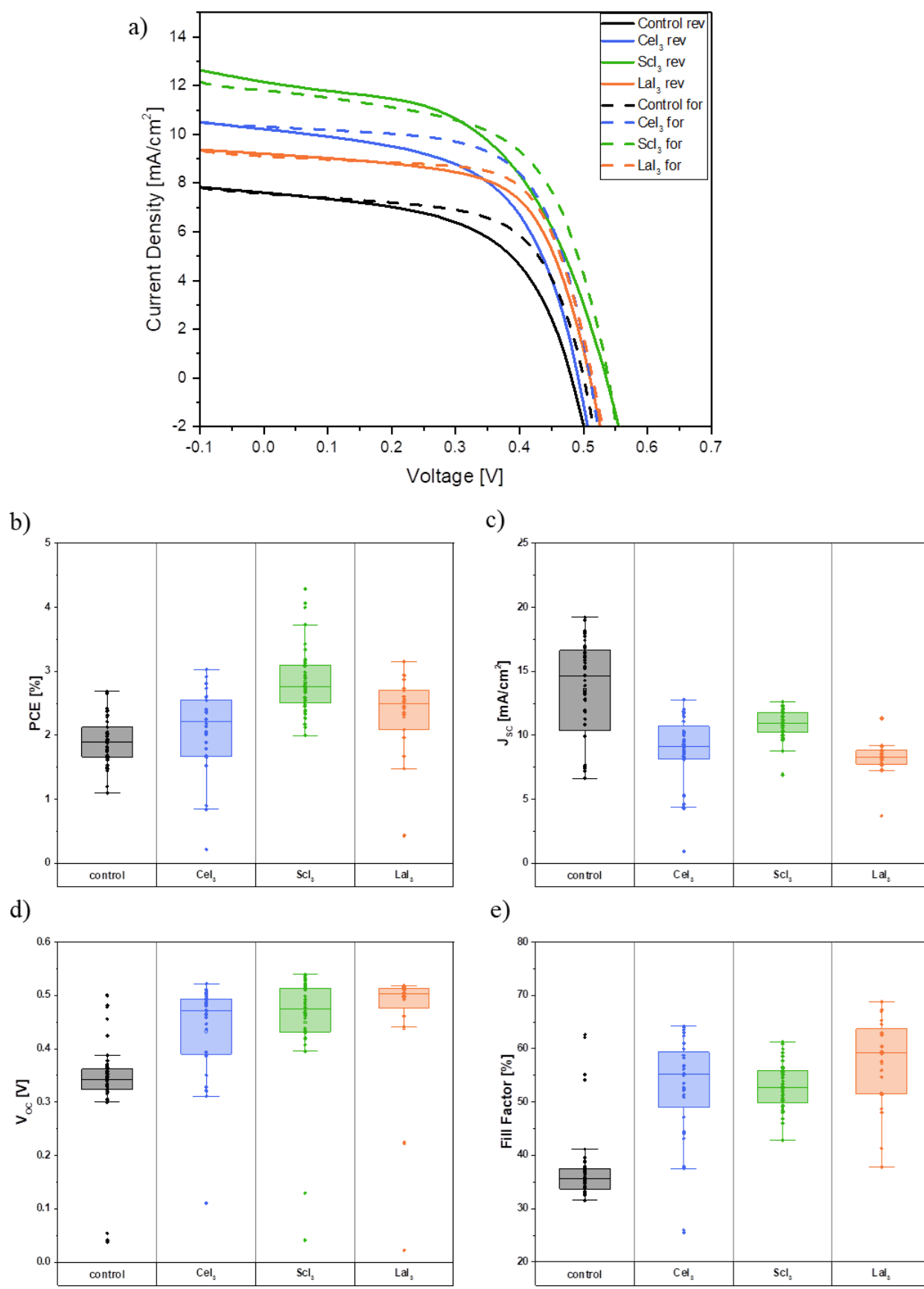
Figure 3. a) JV characteristic for the champion device of each composition; b-d) Box Plot of the

photovoltaic parameters for the control and doped device,

The photovoltaic performances of the thin films have then been investigated by preparing p-i-n devices with ITO/PEDOT:PSS/Perovskite/C60/BCP/Ag structure. In Figure 3a we report the JV curves of best performing devices for control and doped samples while Figures 3b-d show the box plots of measured photovoltaic parameters for a series of fabricated devices. Despite no device optimization was carried out, our results demonstrate the improvement in photovoltaic parameters for all the trivalent-doped samples compared to the control device. It is further interesting to notice that La- and Sc-doped thin films deliver superior photovoltaic efficiency compared to Ce-doped samples, with a significant improvement of V_{OC}, consistent with the similar conductivity reduction exhibited by these two dopants, despite showing opposite PL trend. Considering the best performing devices, Sc-doped films improve both J_{SC} and V_{OC}, suggesting a reduction of p-doping and of trap assisted recombination, respectively, compared to the pristine material,[29] confirming the DFT analysis.

In summary, the limited efficiency of THPs stems from challenges in controlling their electrical and defect properties. Our investigation implies the potential modification of self-doping and charge carrier distribution through the precise introduction of specific trivalent dopants. We showed that doping with trivalent ions impacts both the material's electrical properties and recombination processes going beyond typical divalent doping, which mainly affects carrier density and possibly crystal growth. Such findings are pivotal for enhancing the functionality and versatility of perovskite materials, particularly in the field of optoelectronics.

Author information

Luca Gregori - Department of Chemistry, Biology and Biotechnology, University of Perugia, Via Elce di Sotto 8, 06123, Perugia, Italy. https://orcid.org/0000-0002-0023-8313

Chiara Frasca - Helmholtz-Zentrum Berlin für Materialien und Energie GmbH, Hahn-Meitner Platz 1, 14109 Berlin, Germany.

Daniele Meggiolaro - Computational Laboratory for Hybrid/Organic Photovoltaics (CLHYO), Istituto CNR di Scienze e Tecnologie Chimiche "'Giulio Natta'" (CNR-SCITEC), Via Elce di Sotto 8, 06123 Perugia, Italy. https://orcid.org/0000-0001-9717-133X

Paola Belanzoni - Department of Chemistry, Biology and Biotechnology, University of Perugia, Via Elce di Sotto 8, 06123, Perugia, Italy https://orcid.org/0000-0002-1286-9294

Muhammad Waqar Ashraf - Department of Mechanical Engineering, College of Engineering, Prince Mohammad Bin Fahd University, P.O. Box 1664, Al Khobar, 31952, Saudi Arabia.

Artem Musiienko - Helmholtz-Zentrum Berlin für Materialien und Energie GmbH, Hahn-Meitner Platz 1, 14109 Berlin, Germany.

Antonio Abate - Helmholtz-Zentrum Berlin für Materialien und Energie GmbH, Hahn-Meitner Platz 1, 14109 Berlin, Germany; Department of Chemical, Materials and Production Engineering, University of Naples Federico II, Piazzale Tecchio 80, 80125 Fuorigrotta, Italy.

Filippo De Angelis - Department of Chemistry, Biology and Biotechnology, University of Perugia, Via Elce di Sotto 8, 06123, Perugia, Italy; Department of Mechanical Engineering, College of Engineering, Prince Mohammad Bin Fahd University, P.O. Box 1664, Al Khobar, 31952, Saudi

Arabia. SKKU Institute of Energy Science and Technology (SIEST) Sungkyunkwan University, Suwon, Korea 440-746. https://orcid.org/0000-0003-3833-1975

References

(1) Kojima, A.; Teshima, K.; Shirai, Y.; Miyasaka, T. Organometal Halide Perovskites as Visible-Light Sensitizers for Photovoltaic Cells. *J. Am. Chem. Soc.* **2009**, *131* (17), 6050–6051. https://doi.org/10.1021/ja809598r.

(2) Lee, M. M.; Teuscher, J.; Miyasaka, T.; Murakami, T. N.; Snaith, H. J. Efficient Hybrid Solar Cells Based on Meso-Superstructured Organometal Halide Perovskites. *Science* **2012**, *338* (6107), 643–647. https://doi.org/10.1126/science.1228604.

(3) Kim, H.-S.; Lee, C.-R.; Im, J.-H.; Lee, K.-B.; Moehl, T.; Marchioro, A.; Moon, S.-J.; Humphry-Baker, R.; Yum, J.-H.; Moser, J. E.; Grätzel, M.; Park, N.-G. Lead Iodide Perovskite Sensitized All-Solid-State Submicron Thin Film Mesoscopic Solar Cell with Efficiency Exceeding 9%. *Sci. Rep.* **2012**, *2* (1), 591. https://doi.org/10.1038/srep00591.

(4) Chung, I.; Lee, B.; He, J.; Chang, R. P. H.; Kanatzidis, M. G. All-Solid-State Dye-Sensitized Solar Cells with High Efficiency. *Nature* **2012**, *485* (7399), 486–489. https://doi.org/10.1038/nature11067.

(5) Liang, Z.; Zhang, Y.; Xu, H.; Chen, W.; Liu, B.; Zhang, J.; Zhang, H.; Wang, Z.; Kang, D.-H.; Zeng, J.; Gao, X.; Wang, Q.; Hu, H.; Zhou, H.; Cai, X.; Tian, X.; Reiss, P.; Xu, B.; Kirchartz, T.; Xiao, Z.; Dai, S.; Park, N.-G.; Ye, J.; Pan, X. Homogenizing Out-of-Plane Cation Composition in Perovskite Solar Cells. *Nature* **2023**, *624* (7992), 557–563. https://doi.org/10.1038/s41586-023-06784-0.

(6) Li, H.; Zhang, W. Perovskite Tandem Solar Cells: From Fundamentals to Commercial Deployment. *Chem. Rev.* **2020**, *120* (18), 9835–9950. https://doi.org/10.1021/acs.chemrev.9b00780.

(7) Lin, R.; Wang, Y.; Lu, Q.; Tang, B.; Li, J.; Gao, H.; Gao, Y.; Li, H.; Ding, C.; Wen, J.; Wu, P.; Liu, C.; Zhao, S.; Xiao, K.; Liu, Z.; Ma, C.; Deng, Y.; Li, L.; Fan, F.; Tan, H. All-Perovskite Tandem Solar Cells with 3D/3D Bilayer Perovskite Heterojunction. *Nature* **2023**, *620* (7976), 994–1000. https://doi.org/10.1038/s41586-023-06278-z.

(8) Tong, J.; Jiang, Q.; Zhang, F.; Kang, S. B.; Kim, D. H.; Zhu, K. Wide-Bandgap Metal Halide Perovskites for Tandem Solar Cells. *ACS Energy Lett.* **2021**, *6* (1), 232–248. https://doi.org/10.1021/acsenergylett.0c02105.

(9) Nasti, G.; Abate, A. Tin Halide Perovskite (ASnX$_3$) Solar Cells: A Comprehensive Guide toward the Highest Power Conversion Efficiency. *Adv. Energy Mater.* **2020**, *10* (13), 1902467. https://doi.org/10.1002/aenm.201902467.

(10) K. Noel, N.; D. Stranks, S.; Abate, A.; Wehrenfennig, C.; Guarnera, S.; Haghighirad, A.-A.; Sadhanala, A.; E. Eperon, G.; K. Pathak, S.; B. Johnston, M.; Petrozza, A.; M. Herz, L.; J. Snaith, H. Lead-Free Organic–Inorganic Tin Halide Perovskites for Photovoltaic Applications. *Energy Environ. Sci.* **2014**, *7* (9), 3061–3068. https://doi.org/10.1039/C4EE01076K.

(11) Milot, R. L.; Klug, M. T.; Davies, C. L.; Wang, Z.; Kraus, H.; Snaith, H. J.; Johnston, M. B.; Herz, L. M. The Effects of Doping Density and Temperature on the Optoelectronic Properties of Formamidinium Tin Triiodide Thin Films. *Adv. Mater.* **2018**, *30* (44), 1804506. https://doi.org/10.1002/adma.201804506.

(12) Meggiolaro, D.; Ricciarelli, D.; Alasmari, A. A.; Alasmary, F. A. S.; De Angelis, F. Tin versus Lead Redox Chemistry Modulates Charge Trapping and Self-Doping in Tin/Lead Iodide

Perovskites. *J. Phys. Chem. Lett.* **2020**, *11* (9), 3546–3556. https://doi.org/10.1021/acs.jpclett.0c00725.

(13) Ricciarelli, D.; Meggiolaro, D.; Ambrosio, F.; De Angelis, F. Instability of Tin Iodide Perovskites: Bulk p-Doping versus Surface Tin Oxidation. *ACS Energy Lett.* **2020**, *5* (9), 2787–2795. https://doi.org/10.1021/acsenergylett.0c01174.

(14) Pascual, J.; Flatken, M.; Félix, R.; Li, G.; Turren-Cruz, S.-H.; Aldamasy, M. H.; Hartmann, C.; Li, M.; Di Girolamo, D.; Nasti, G.; Hüsam, E.; Wilks, R. G.; Dallmann, A.; Bär, M.; Hoell, A.; Abate, A. Fluoride Chemistry in Tin Halide Perovskites. *Angew. Chem. Int. Ed.* **2021**, *60* (39), 21583–21591. https://doi.org/10.1002/anie.202107599.

(15) Meggiolaro, D.; Gregori, L.; De Angelis, F. Formation of a Mixed Valence Sn_3F_8 Phase May Explain the SnF_2 Stabilizing Role in Tin-Halide Perovskites. *ACS Energy Lett.* **2023**, *8* (5), 2373–2375. https://doi.org/10.1021/acsenergylett.3c00652.

(16) Abate, A. Stable Tin-Based Perovskite Solar Cells. *ACS Energy Lett.* **2023**, *8* (4), 1896–1899. https://doi.org/10.1021/acsenergylett.3c00282.

(17) a) Jiang, X.; Li, H.; Zhou, Q.; Wei, Q.; Wei, M.; Jiang, L.; Wang, Z.; Peng, Z.; Wang, F.; Zang, Z.; Xu, K.; Hou, Y.; Teale, S.; Zhou, W.; Si, R.; Gao, X.; Sargent, E. H.; Ning, Z. One-Step Synthesis of SnI2·(DMSO)x Adducts for High-Performance Tin Perovskite Solar Cells. *J. Am. Chem. Soc.* **2021**, *143* (29), 10970–10976. https://doi.org/10.1021/jacs.1c03032; b) Chen, J.; Luo, J.; Hou, E.; Song, P.; Li, Y.; Sun, C.; Feng, W.; Cheng, S.; Zhang, H.; Xie,L.; Tian, C.; Wei, Z. Efficient tin-based perovskite solar cells with trans-isomeric fulleropyrrolidine additives *Nat. Photon.* **2024**, https://doi.org/10.1038/s41566-024-01381-7 .

(18) Lanzetta, L.; Gregori, L.; Hernandez, L. H.; Sharma, A.; Kern, S.; Kotowska, A. M.; Emwas, A.-H.; Gutiérrez-Arzaluz, L.; Scurr, D. J.; Piggott, M.; Meggiolaro, D.; Haque, M. A.; De Angelis, F.; Baran, D. Dissociative Host-Dopant Bonding Facilitates Molecular Doping in Halide Perovskites. *ACS Energy Lett.* **2023**, *8* (7), 2858–2867. https://doi.org/10.1021/acsenergylett.3c00818.

(19) Zhao, P.; Yin, W.; Kim, M.; Han, M.; Song, Y. J.; Ahn, T. K.; Jung, H. S. Improved Carriers Injection Capacity in Perovskite Solar Cells by Introducing A-Site Interstitial Defects. *J. Mater. Chem. A* **2017**, *5* (17), 7905–7911. https://doi.org/10.1039/C7TA01203A.

(20) Cao, J.; Tao, S. X.; Bobbert, P. A.; Wong, C.; Zhao, N. Interstitial Occupancy by Extrinsic Alkali Cations in Perovskites and Its Impact on Ion Migration. *Adv. Mater.* **2018**, *30* (26), 1707350. https://doi.org/10.1002/adma.201707350.

(21) Sabino, F. P.; Zunger, A.; Dalpian, G. M. Intrinsic Doping Limitations in Inorganic Lead Halide Perovskites. *Mater. Horiz.* **2022**, *9* (2), 791–803. https://doi.org/10.1039/D1MH01371H.

(22) Lyons, J. L. Effective Donor Dopants for Lead Halide Perovskites. *Chem. Mater.* **2021**, *33* (15), 6200–6205. https://doi.org/10.1021/acs.chemmater.1c01898.

(23) Zhou, C.; Zhang, T.; Zhang, C.; Liu, X.; Wang, J.; Lin, J.; Chen, X. Unveiling Charge Carrier Recombination, Extraction, and Hot‐Carrier Dynamics in Indium Incorporated Highly Efficient and Stable Perovskite Solar Cells. *Adv. Sci.* **2022**, *9* (11), 2103491. https://doi.org/10.1002/advs.202103491.

(24) Mosconi, E.; Merabet, B.; Meggiolaro, D.; Zaoui, A.; De Angelis, F. First-Principles Modeling of Bismuth Doping in the $MAPbI_3$ Perovskite. *J. Phys. Chem. C* **2018**, *122* (25), 14107–14112. https://doi.org/10.1021/acs.jpcc.8b01307.

(25) Hao, F.; Stoumpos, C. C.; Cao, D. H.; Chang, R. P. H.; Kanatzidis, M. G. Lead-Free Solid-State Organic–Inorganic Halide Perovskite Solar Cells. *Nat. Photonics* **2014**, *8* (6), 489–494. https://doi.org/10.1038/nphoton.2014.82.

(26) Nasti, G.; Aldamasy, M. H.; Flatken, M. A.; Musto, P.; Matczak, P.; Dallmann, A.; Hoell, A.; Musiienko, A.; Hempel, H.; Aktas, E.; Di Girolamo, D.; Pascual, J.; Li, G.; Li, M.; Mercaldo, L. V.; Veneri, P. D.; Abate, A. Pyridine Controlled Tin Perovskite Crystallization. *ACS Energy Lett.* **2022**, *7* (10), 3197–3203. https://doi.org/10.1021/acsenergylett.2c01749.

(27) Di Girolamo, D.; Blundo, E.; Folpini, G.; Ponti, C.; Li, G.; Aldamasy, M. H.; Iqbal, Z.; Pascual, J.; Nasti, G.; Li, M.; Avolio, R.; Russina, O.; Latini, A.; Alharthi, F.; Felici, M.; Petrozza, A.; Polimeni, A.; Abate, A. Energy Distribution in Tin Halide Perovskite. *Sol. RRL* **2022**, *6* (8), 2100825. https://doi.org/10.1002/solr.202100825.

(28) Savill, K. J.; Ulatowski, A. M.; Herz, L. M. Optoelectronic Properties of Tin–Lead Halide Perovskites. *ACS Energy Lett.* **2021**, *6* (7), 2413–2426. https://doi.org/10.1021/acsenergylett.1c00776.

(29) Aldamasy, M. H.; Musiienko, A.; Rusu, M.; Regaldo, D.; Zho, S.; Hampel, H.; Frasca, C.; Iqbal, Z.; Gries, T. W.; Li, G.; Aktas, E.; Nasti, G.; Li, M.; Pascual, J.; Hartono, N. T. P.; Wang, Q.; Unold, T.; Abate, A. Photovoltaic Potential of Tin Perovskites Revealed through Layer-by-Layer Investigation of Optoelectronic and Charge Transport Properties. **2023**. https://doi.org/10.48550/ARXIV.2309.05481.

(30) Lee, S. J.; Shin, S. S.; Kim, Y. C.; Kim, D.; Ahn, T. K.; Noh, J. H.; Seo, J.; Seok, S. I. Fabrication of Efficient Formamidinium Tin Iodide Perovskite Solar Cells through SnF$_2$–Pyrazine Complex. *J. Am. Chem. Soc.* **2016**, *138* (12), 3974–3977. https://doi.org/10.1021/jacs.6b00142.

(31) Chen, Q.; Luo, J.; He, R.; Lai, H.; Ren, S.; Jiang, Y.; Wan, Z.; Wang, W.; Hao, X.; Wang, Y.; Zhang, J.; Constantinou, I.; Wang, C.; Wu, L.; Fu, F.; Zhao, D. Unveiling Roles of Tin Fluoride Additives in High-Efficiency Low-Bandgap Mixed Tin-Lead Perovskite Solar Cells. *Adv. Energy Mater.* **2021**, *11* (29), 2101045. https://doi.org/10.1002/aenm.202101045.